Compression Testing using a Cam-Driven Electromagnetic Machine

C.M.A Silva[1], P.A.R. Rosa[1], P.A.F. Martins[1]

[1] IDMEC, Instituto Superior Técnico, Technical University of Lisbon, Portugal

Abstract

This paper presents new equipment for the compression testing of materials under high rates of loading. The equipment consists of an electromagnetic actuator, a fixed housing containing two flat compression platens, a translating cam and a follower. The electromagnetic actuator makes possible reaching high strain rates with a very precise control of the impact velocity and of the energy transmitted to the translating cam. The cam profile enables compression testing to be performed under the strain-rate vs. strain loading paths that are commonly found in manufacturing in order to meet the machine-tool and process combined specifications. The equipment was designed, fabricated and instrumented by the authors and, besides giving constructive details for those readers that may be interested in developing a low-cost equipment for compression testing at high rates of loading, the paper also puts emphasis on the flexibility and adequacy of its operative conditions for determining the mechanical behaviour of Aluminium AA1050-O under different testing conditions.

Keywords

Compression testing, Electromagnetic, Flow curve.

1 Introduction

The flow curve at the appropriate rates of loading is very important to describe the hardening behaviour during plastic deformation in terms of strain, strain-rate and temperature, to set-up the non-linear constitutive equations of metal plasticity and to establish the feasibility window and effectiveness of manufacturing processes. However, despite this importance, the flow curve is not always accessible in conditions similar to real manufacturing due to difficulties in replicating the operative conditions, namely the combined evolution and range of strains and strain-rates.

In case of strain-rates, for example, the widely available universal testing machines can only perform mechanical characterization of materials at quasi-static or low rate

loading conditions ($\dot{\bar{\varepsilon}}$~10^{-3} to 10 s^{-1}) and commercially available drop weight testing systems are only adequate for medium rates of loading ($\dot{\bar{\varepsilon}}$~1 to 10^3 s^{-1}). Special purpose testing equipment based on split Hopkinson pressure bars, which is adequate for high rates of loading ($\dot{\bar{\varepsilon}}$~10^3 to 10^4 s^{-1}), and Taylor impact systems, which are necessary for even higher rates of loading ($\dot{\bar{\varepsilon}}$ > 10^4 s^{-1}), are not readily available to purchase or guaranteed to the majority of researchers.

However, even if equipment for testing at high rates of loading is available, a frequently ignored and mismanaged technical issue is the adequacy of testing conditions to the operational settings of the machine-tools where manufacturing processes will take place. In fact, despite theoretical claims on transferability of results often requiring mechanical testing of materials with different strain and strain-rate loading profiles to provide the same stress response for a given value of strain and strain rate, it is known that the flow curves obtained under testing with unclear conditions lead to non-unique and non-representative responses for the same material [1]. Not only time history of strain and strain-rate influences stress response [2] as it is relevant to determine crystallographic textures resulting from manufacturing processes [3].

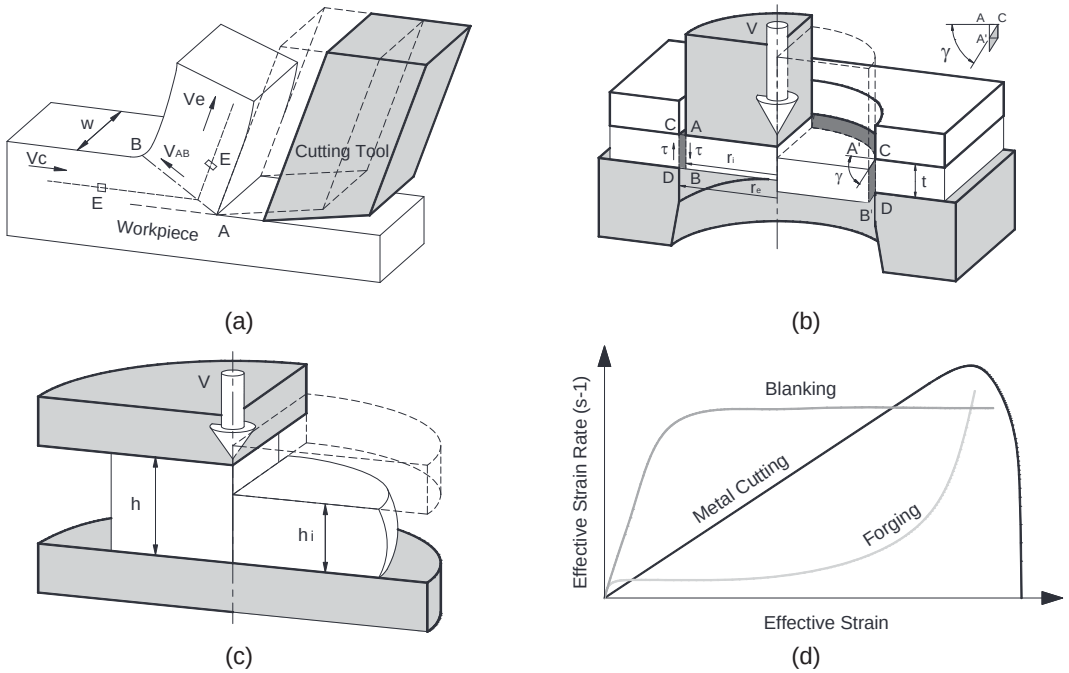

Figure 1: *(a) Metal cutting, (b) blanking and (c) forging together with a schematic representation of the (d) corresponding strain-rate vs. strain loading paths.*

As a result of this, mechanical characterization of materials requires a deep insight into the machines and deformation mechanics of the processes prior to choosing the most appropriate equipment and operative testing conditions [4]. Taking metal cutting as an example, the synergism between the mechanical behaviour of materials and the machine-tools requires a good understanding of the displacement-time relationship of the cutting tool and of its influence in the rate dependent variables of the process. Because strain-rate growths with the level of strain as material moves from the undeformed region to the shear plane (a very narrow plastic deformation zone around AB in Figure 1a) and decreases while material moves away from the shear plane up the rake face of the tool,

the resulting strain-rate vs. strain loading path for a typical flow route (refer to E in Figure 1a) is plotted in Figure 1d.

This means that the typical strain-rate vs. strain loading paths of metal cutting are significantly different from those obtained with commercially available testing equipment for medium and high rates of loading. In case of split Hopkinson pressure bars, for example, strain-rate vs. strain loading paths are characterized by an approximately constant level of strain-rate [5], similar to that plotted for blanking in Figures 1b and 1d, while in case of drop-height testing systems the strain-rate vs. strain loading paths are similar to that of forging (Figures 1c and 1d).

The abovementioned difficulties in obtaining the flow curves at appropriate rates of loading and the aforesaid synergism between material testing and real manufacturing conditions, justify the following two-fold objective of this paper; (i) the development of an innovative cam-driven electromagnetic machine for the compression testing of materials under high rates of loading and (ii) the identification of new testing methodologies based on the selection of the strain-rate vs. strain loading paths that can easily and effectively replicate the strain-rate vs. strain loading paths found in real manufacturing.

2 Cam-Driven Electromagnetic Testing Machine

Figure 2 shows the equipment that was designed and fabricated by the authors. Three main groups of components can be identified; (i) basic structural parts, (ii) specific mechanical parts and (iii) specific electrical and electromagnetic parts. The design of the basic and specific parts will be described in what follows.

2.1 Basic Structural Parts

Basic structural parts comprise the support frame and fixing accessories that are independent of the type of testing conditions and materials to be characterized. The support frame accounts for the installation of the specific mechanical, electrical and electromagnetic parts. The overall length of the frame was chosen so that larger compression housings and longer actuators can be added in the future with the objective of enlarging the size of the test specimens and increasing the velocity and kinetic energy of the ram.

2.2 Specific Mechanical Parts

Specific mechanical parts comprise a fixed housing containing two flat compression platens, a translating cam and a follower whose design depends on the operative conditions of manufacturing to be replicated.

The compression platens are made from a cold working tool steel DIN 120WV4 hardened and tempered to 60 HRc. The translating cam and the follower are made from steel DIN 14NiCr14 and DIN 100Cr6, respectively. The clearance fit for the cam-follower system is H7/f7 (ISO) and the individual parts were manufactured in a CNC machining centre. Final manual grinding and polishing was necessary to eliminate small surface errors and imperfections that although being imperceptible to eye could cause high stress and vibrations in the cam follower. Protection of the sliding elements of the cam system was performed by means of a PTFE (Teflon added) oil based lubricant.

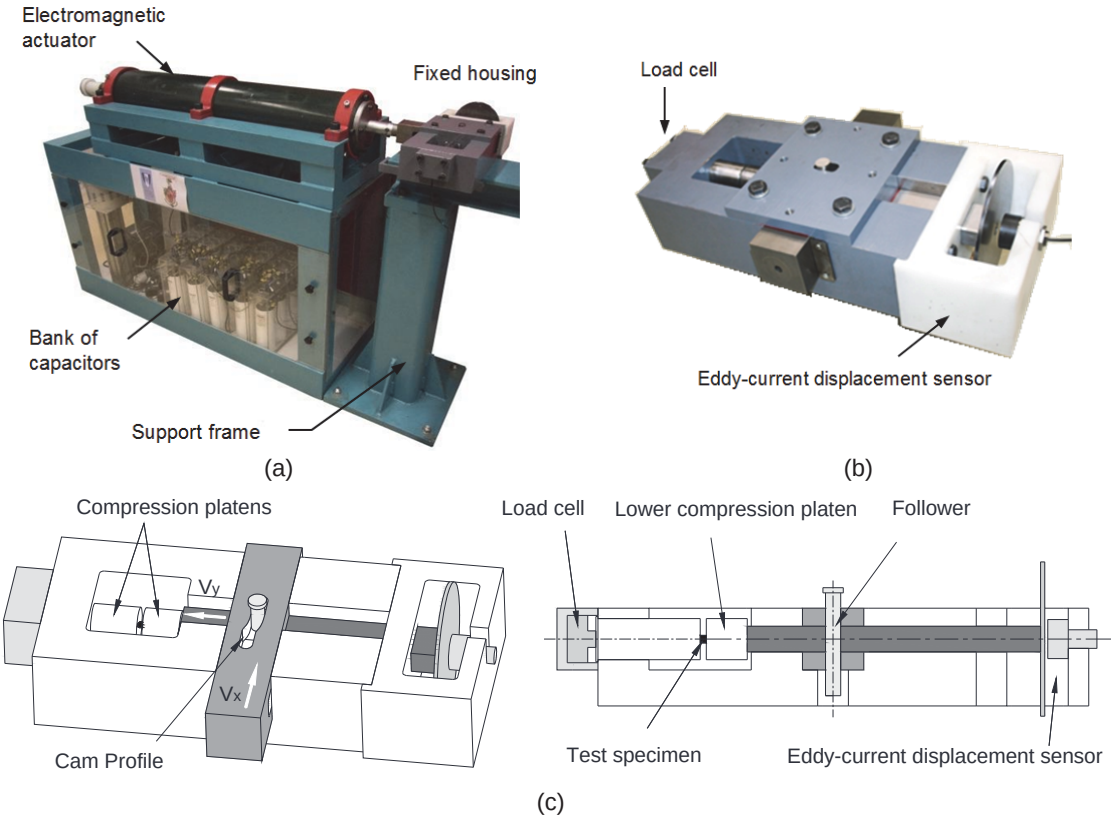

Figure 2: *(a) Cam-driven electromagnetic testing machine, (b) detail of the fixed housing and (c) schematic drawing showing the translating cam, the follower, the compression platens, the load cell and the displacement sensor.*

The surface contour of the cam (cam profile) is to be designed with the objective of synchronizing the performance of the testing machine with that of the machine-tool where manufacturing will take place. The follower traces the cam profile and converts horizontal movement (x) of the ram to vertical displacement (y) of the lower compression platen (Figure 2c). The conversion of movement is schematically illustrated in Figure 3a.

In case of the cam shown in Figure 3b, the profile (hereafter designated as 'logistic profile') is characterized by an entry dwell followed by a rise contour and a final dwell towards the uppermost profile of the cam. The vertical displacement y of the follower as a function of the horizontal displacement x of the ram is depicted in Figure 3c.

The velocity v_y of the follower is directly related to the first derivative of the displacement curve because the velocity of the ram v_x is approximately constant in the working region of the cam follower (v_x^{avg}=10 m/s), refer to the region located in-between the dashed vertical lines in Figure 3d),

$$v_y = \frac{dy}{dt} = v_x \frac{dy}{dx} \cong v_x^{avg} \frac{dy}{dx} \tag{1}$$

The leftmost region in Figure 3d, characterized by a sharp increase in the velocity of the ram, results from the initial acceleration due to the pressure generated by the coils inside the electromagnetic actuator. There is no vertical movement of the cam follower along this region and, therefore, there is no compression of the upset test specimen. The rightmost region in Figure 3d unveils part of the deceleration of the ram after the follower

has reached the uppermost profile of the cam. Again, there is no compression of the upset test specimen along this region.

As a result of this, the vertical movement of the cam follower leading to upset compression only takes place at the region placed in-between the dashed vertical lines in Figure 3d, hereafter named as the 'working region of the cam profile'. This justifies the reason why subsequent figures showing the displacement of the ram as the horizontal axis (x-axis) are frequently limited to the working region of the cam profile.

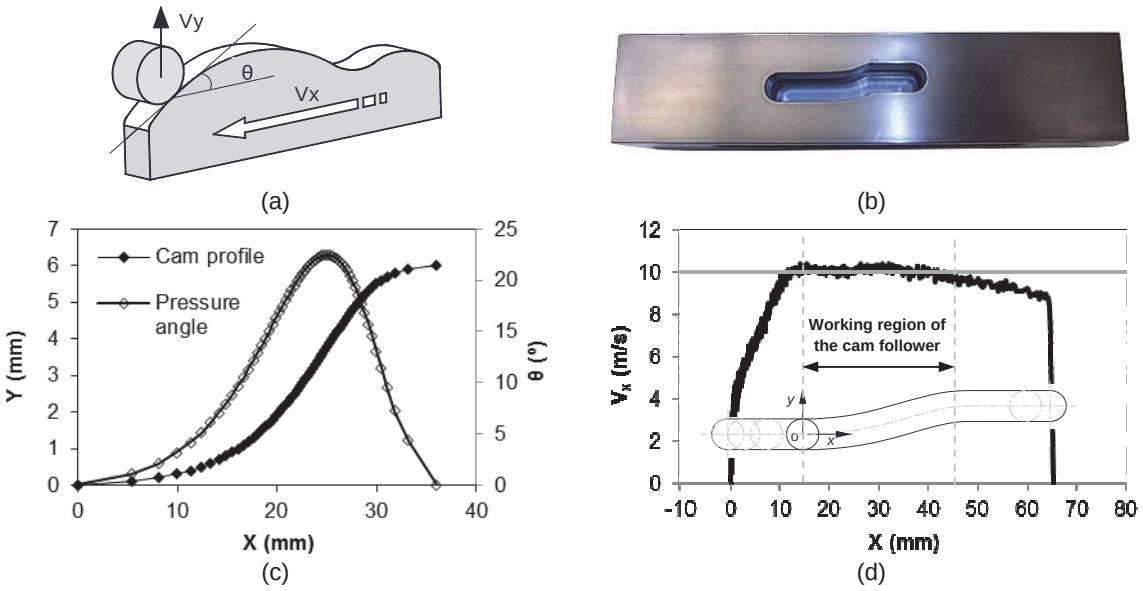

Figure 3: *(a) Schematic representation of the cam profile and follower, (b) photograph of the logistic cam, (c) cam profile and pressure angle and (d) velocity of the ram* v_x^{avg} *=10 m/s in the working region of the cam follower.*

The acceleration a_y of the cam follower is computed from the variation in the velocity v_y (assuming the above mentioned approximation of v_x) and the kinematic analysis of the follower shown in Figure 4a allows us to conclude that the cam utilized in the experiments provides the maximum velocity at the point of inflection located near the maximum slope of the cam profile.

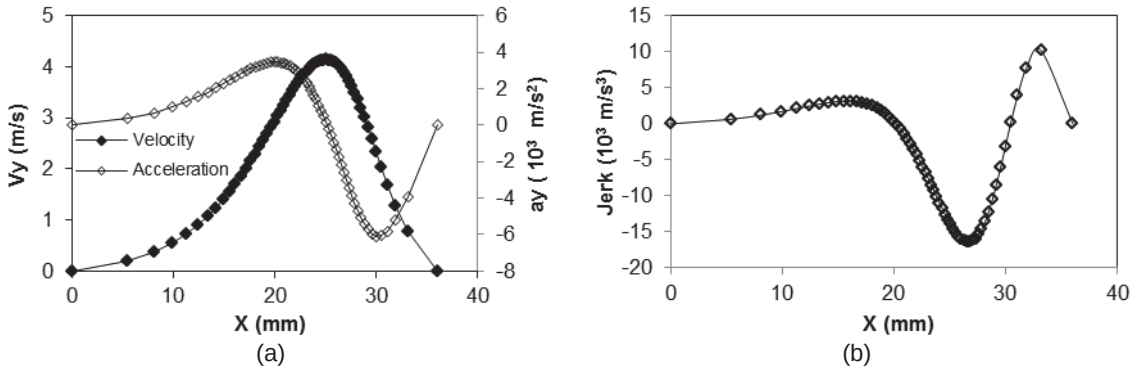

Figure 4: *(a) Velocity and acceleration of the follower and (b) jerk in the working region of the cam-driven electromagnetic testing machine equipped with a logistic cam.*

Acceleration is approximately constant at the entry dwell of the cam profile and presents an abrupt change from positive and to negative values at the midpoint. Along the entry dwell of the cam, jerk is approximately null (Figure 4b).

The small values of acceleration at the entry dwell of the logistic cam profile combined with the fact that pressure angles θ of the follower are kept below 30º [6] (θ^{max} =22.5º, Figure 3c), help keeping inertia forces at a small level and justify the reason why the proposed testing equipment worked smoothly without shocks and vibrations while performing material testing at high rates of loading.

The logistic cam profile allows replicating material flow conditions in conditions similar to those found in metal cutting processes [5]. However, because the cam system is flexible and its profile depends on the operative conditions to be replicated, it is easy to change the kinematics of the proposed equipment in order to replicate another manufacturing process, machine-tool or material testing equipment. For instance, replacing the logistic cam by a 'root type cam' allows the machine to replicate the kinematics of a split Hopkinson pressure bar (Figure 5).

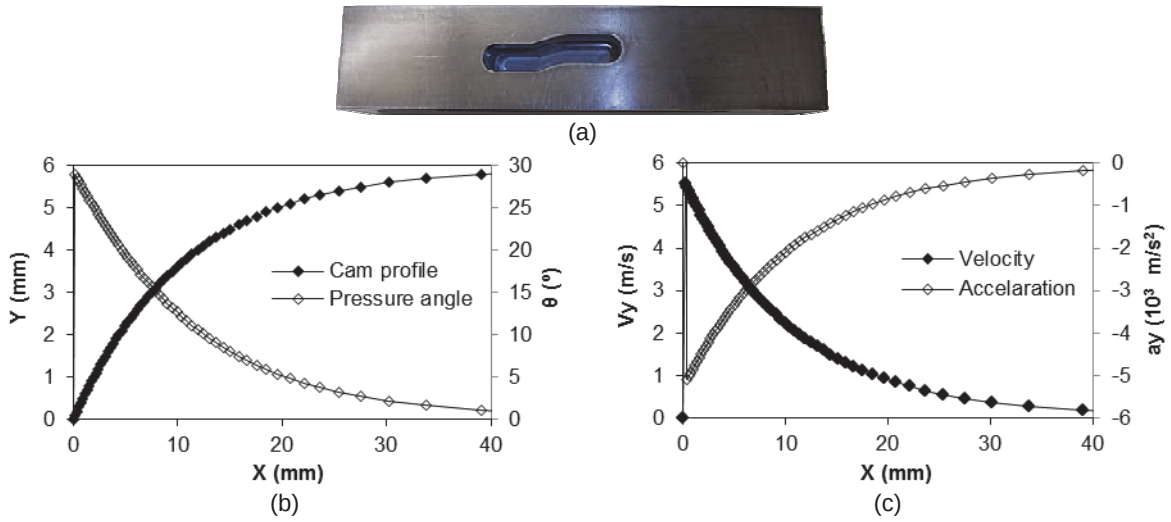

Figure 5: *(a) Photograph of the root type cam, (b) cam profile and pressure angle and (c) velocity and acceleration of the follower in the working region of the cam-driven electromagnetic testing machine equipped with a root type cam.*

2.3 Specific Electric and Electromagnetic Parts

Specific electrical and electromagnetic parts include the eddy-current displacement sensor, the force transducer and the components that provide the energy to the electromagnetic actuator, e.g. the electrical circuits for charging and firing the bank of capacitors and the coils that generate the pressure for accelerating the ram linked to one end of the translating cam.

The vertical movement of the cam follower is transformed into compression of the test specimen via the lower flat platen. The vertical displacement of the lower flat platen is measured by a eddy-current displacement sensor and the resulting force is measured by means of a load cell connected to the upper compression platen (Figure 2c).

The electromagnetic actuator consists of electrical circuits for charging and firing the banks of energy-storage capacitors (each with 6 mF) and a series of coils that generate

the pressure to accelerate the ram linked to the translating cam. Typical coils with eight windings, a total length of 92 mm, an external diameter of 160 mm and an internal diameter of 70 mm, were utilized. The ram consists of a long (1.5 m) and heavy (5.2 kg) bimetallic bar made of AA 6082-T651 Aluminium with slotted hollow half-ring surface inserts (to reduce eddy current losses) of DIN St52.3 Steel (Figure 6).

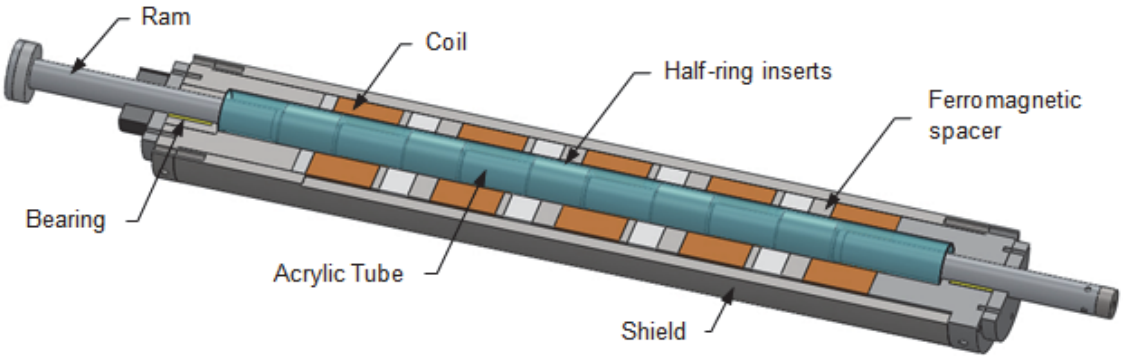

Figure 6: *Electromagnetic actuator showing the ram, the coils, the half-ring inserts and the ferromagnetic spacers.*

The capacitors are charged by means of single-phase alternating current supplied with 230 V that is converted to higher-voltage direct constant current by means of a charging circuit consisting of a variable-voltage transformer (capable of producing 3.6 times the input voltage) and a constant current rectifier system. Once the capacitors are charged, the charging circuits are closed and the thyristor switches located in the discharging circuits are activated to simultaneously fire each capacitor into its associated coil. The resulting current pulse will only last for a few miliseconds but the amount of time will be enough for accelerating the ram to levels of velocity up to 18 m/s.

3 Experimental Procedure

The stress-strain curve of Aluminium AA1050-O was obtained by means of compression tests on cylindrical specimens with 6 mm diameter and 6 mm height. Both logistic and root type cam profiles were utilized (Table 1). The quasi-static conditions were included as a reference.

Case	Testing Conditions	Vx	Case	Testing Conditions	Vx
1	Quasi-static	0.01	7	Root type cam profile	3.5
2	Logistic cam profile	4	8	Root type cam profile	7
3	Logistic cam profile	3.9	9	Root type cam profile	10.4
4	Logistic cam profile	5.8	10	Root type cam profile	14
5	Logistic cam profile	7.8	11	Root type cam profile	17.5
6	Logistic cam profile	9.2			

Table 1: *The plan of experiments*

4 Results and Discussion

Figure 7 shows the variation of force with displacement obtained from test cases 3 and 8 in Table 1. Results show that on contrary to root type cam profiles (and split Hopkinson pressure bars), there are no 'saw tooth' oscillations when using a logistic cam profile (case 3). This is attributed to a smooth transition between the entry dwell and the profile of the cam and to a low value of the maximum pressure angle (θ^{max} = 22.5º, Figure 3c).

The oscillations in the root type cam profile are attributed to inertia forces and stress wave propagation under impact loading as well as to an initial value of the maximum pressure angle very close to 30º (θ^{max} = 28º, Figure 5b).

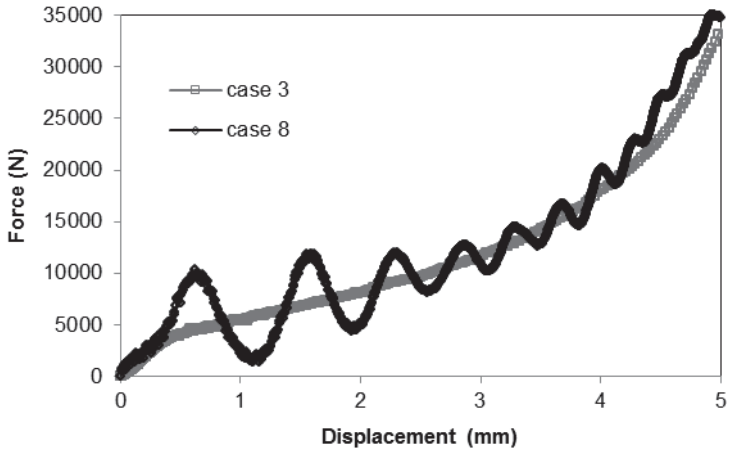

Figure 7: *Experimental evolution of the force vs. displacement for logistic and root type cam profiles.*

The experimental strain-rate vs. strain loading paths for the selected testing conditions performed with the cam-driven electromagnetic testing machine equipped with a logistic cam profile are plotted in Figure 8a.

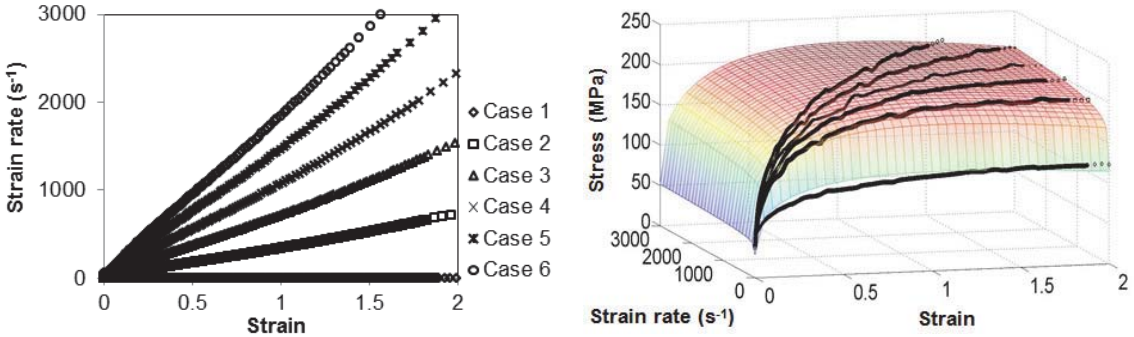

Figure 8: *Mechanical testing of Aluminium AA1050-O using a logistic cam. (a) Strain-rate vs. strain loading paths. (b) Material stress response with respect to strain and strain-rate (experimental data and fitting).*

The three-dimensional flow surface plotted in Figure 8b in which stress, strain and strain-rate are the leading axis results from fitting experimental data to the following mathematical material model that was developed by the authors [5],

$$\sigma = \left(A + e^{m\varepsilon}\varepsilon^{n}\right)\left(B + C\,ln\left[D + \dot{\varepsilon}\right]\right) \tag{2}$$

where, the constants A, B, C, D, m and n are to be determined from experimental data.

The model given by equation (2) is appropriate for cold forming operating conditions and includes well-known material models such as Ludwik-Holloman, Voce and Johnson-Cook (isothermal), among others, as special cases. Another advantage of this model is the ability for exhibiting material flow softening at high values of strain. Flow softening is responsible for diminishing the resistance to plastic deformation due to rearrangement of dislocations under dynamic recrystallization and is known to cause a significant influence in the deformation mechanics of metal cutting, namely chip formation [7].

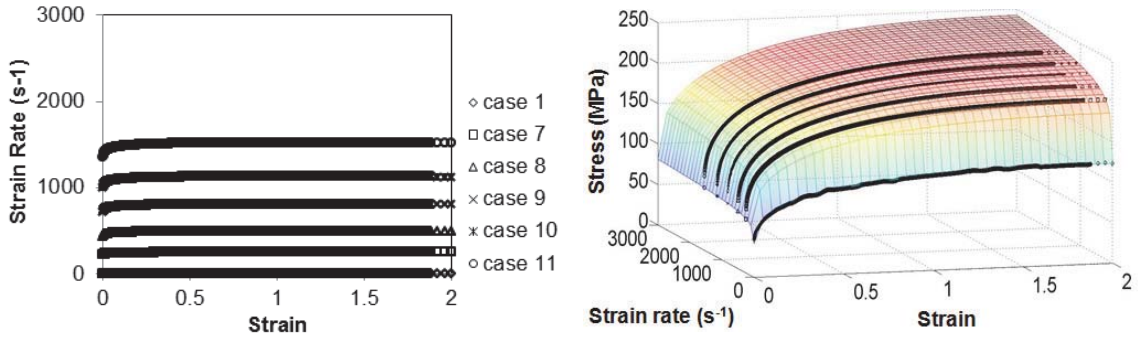

(a) (b)

Figure 9: *Mechanical testing of Aluminium AA1050-O using a root type cam. (a) Strain-rate vs. strain loading paths. (b) Material stress response with respect to strain and strain-rate (experimental data and fitting).*

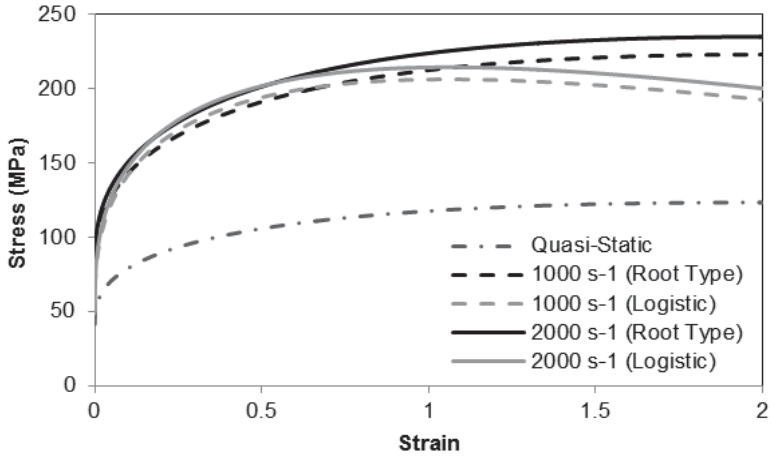

Figure 10: *Experimental stress–strain curves after mathematical fitting for different values of strain-rate.*

Figure 9a provides similar results for the root type cam. As seen, the strain-rate vs. strain loading paths obtained with this type of cam are near horizontal lines and similar to

those commonly attained with Hopkinson pressure bars. The three-dimensional flow surface resulting from these experiments is plotted in Figure 9b.

The differences between the flow surfaces obtained from material testing with logistic and root type cams are made clear by analysing a selection of intersections of the three-dimensional flow surfaces with constant strain-rate planes ($\dot{\bar{\varepsilon}} = Cte$). The flow curves resulting from these intersections are plotted in Figure 10 and indicate that major differences are due to flow softening in close agreement with the aforementioned capability of the logistic cam profile to model metal cutting conditions.

5 Conclusions

The proposed cam-driven electromagnetic testing machine is capable of operating across a broad range of operative conditions found in real manufacturing processes. Variations in cam profiles, modifications in the individual coils of the actuator, which can be easily changed or temporarily switched off during testing, and changes in the operating voltage of the charging and discharging circuits (that influence the kinetic energy of the ram) can be easily and effectively performed in order to achieve different strain vs. strain-rate loading paths.

Experiments show that the proposed machine equipped with a logistic cam is capable of diminishing ‘saw tooth’ oscillations in the experimental recordings of force that are typical of split Hopkinson pressure bars and root type cam profiles. Moreover logistic cam profiles in conjunction with the proposed material model are able to successfully model flow softening that is commonly found in metal cutting applications.

References

[1] *Banabic D., Bunge H.-J., Pöhlandt K., Tekkaya A. E.,* Formability of metallic materials, Springer-Verlag, Berlin, 2000.

[2] *Silva C. M. A., Rosa P. A. R. and Martins P. A. F.,* Mechanical characterization of materials for bulkf using a drop weight testing machine, Journal of Mechanical Engineering Science, 2010, 224, p. 1795-1804.

[3] *Guo Y., Saldana C., Mann J. B., Saoubi R. M., Chandrasek S,* Deformation and microstructure in machining, Advanced Materials Research, 2011, 223, p.325-331.

[4] *Field J. E., Walley S. M., Proud W. G., Goldrein H. T., Siviour C. R.,* Review of experimental techniques for high rate deformation and shock studies, International Journal of Impact Engineering, 2004, 30, p. 725–775.

[5] *Silva C. M. A., Rosa P. A. R., Martins P. A. F.,* Electromagnetic cam driven compression testing equipment”, Experimental Mechanics, 2011 (on-line first).

[6] *Rothbart H. A.,* Cam design handbook. McGraw Hill, New York, 2004.

[7] *Sima M., Özel T.,* Modified material constitutive models for serrated chip formation simulations and experimental validation in machining of titanium alloy Ti-6Al-4V. International Journal of Machine Tools and Manufacture, 2010, 50, p. 943–960.